Journal Name RSCPublishing

ARTICLE

Supplementary Material

Cite this: DOI: 10.1039/x0xx00000x

O. Shindell,[a] N. Mica,[a] M. Ritzer [a] and V. D. Gordon[a] ,

Abstract text goes here. The abstract should be a single paragraph that summarises the content of the article.

Received 00th January 2012,
Accepted 00th January 2012

DOI: 10.1039/x0xx00000x

www.rsc.org/

Supplementary Material

Variation between replicate experiments and possible causes: Within each experiment, the ratio of ordered-phase area to adhering area is roughly constant (Supplementary Figure 2). However, between experiments this ratio varies, as does the frequency distribution of ordered-phase area fractions (Supplementary Figure 2). We also see qualitative differences in the shapes of domains typically seen in different experiments (Supplementary Figure 3). Since these experiments are all done at the same nominal membrane composition, electroformation temperature, and observation temperature, it is clear that one or more thermodynamic parameters is/are varying between experiments.

We tentatively ascribe this to variation in composition, which could arise either from the precision limitations of the Hamilton syringe used for mixing lipid solutions or, more likely, from the formation of unintended amphiphile or protein species during the electroformation process. The presence of unaccounted-for species in the membrane could alter transition temperature, kinetics of phase separation, and the line tension between domains, which is consistent with the differences we see between experiments.

It is also possible that small differences in the rate of cooling could have impinged on the kinetics of phase separation, which could affect domain shape and size for non-equilibrated phase separation. The temperature in our labs is nominally a constant 24 °C, but temperature fluctuations or variations in ambient humidity could affect thermal transfer.

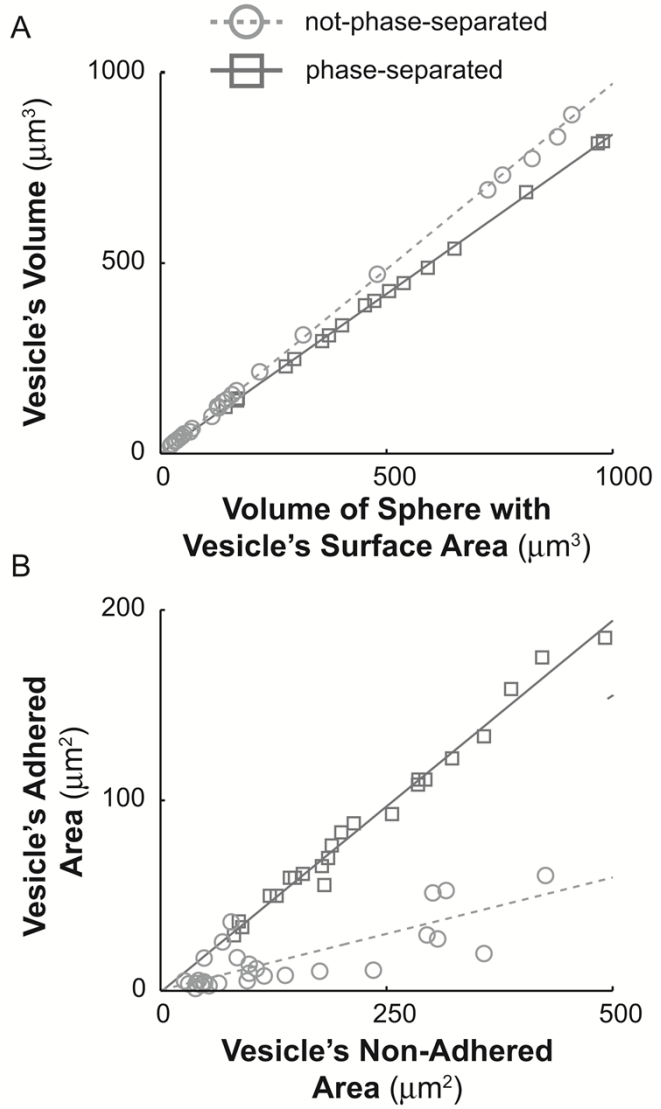

Supplementary Figure 1. Adhered vesicles' geometries have two distinct states: one for phase-separated vesicles and another for not-phase-separated vesicles. A) The ratio of adhered vesicles' volume to the volume of spheres whose surface areas are the same as the vesicles' surface areas. Dark grey squares are phase-separated vesicles with a solid-line fit whose slope is 0.838 ± 0.004 and $R^2 > 0.99$. Light grey circles are not-phase-separated vesicles with a dashed-line fit whose slope is 0.975 ± 0.005 and $R^2 > 0.99$. B) The ratio of adhered vesicles' adhered surface area to the non-adhered surface area. Dark grey squares are phase-separated vesicles with a solid line fit whose slope is 0.39 ± 0.01 and $R^2 > 0.99$. Light grey circles are not-phase-separated vesicles with a dashed-line fit whose slope is 0.13 ± 0.02 and $R^2 > 0.87$. The reported uncertainties in A) and B) are the 95% confidence intervals.

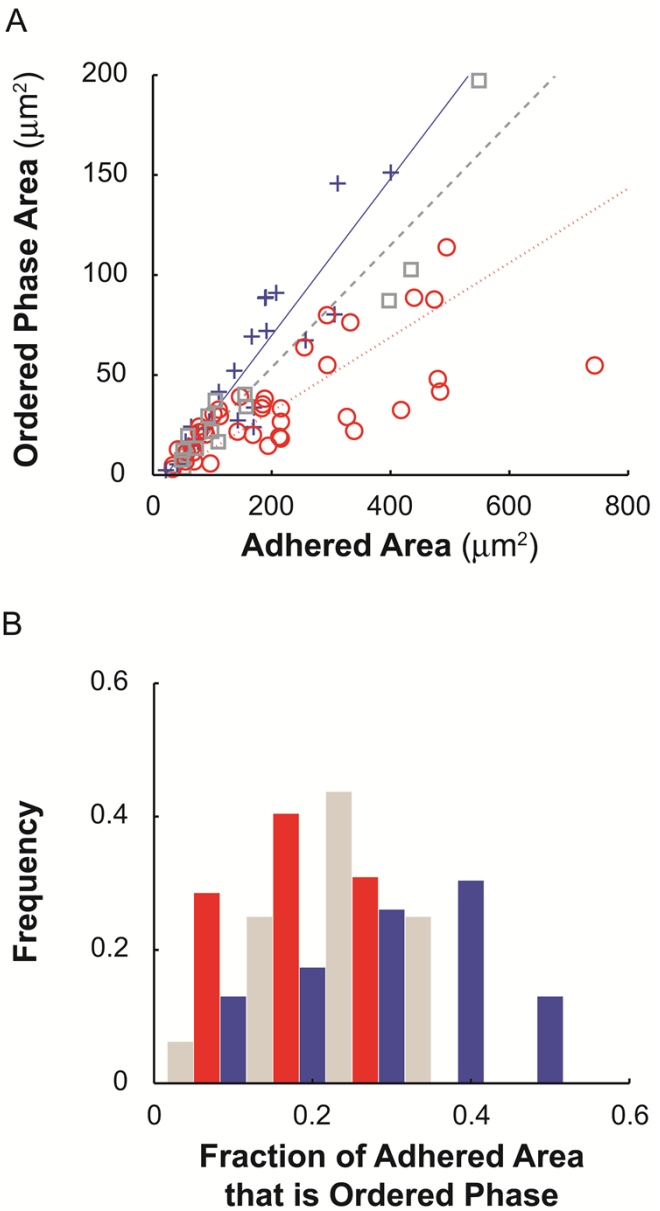

Supplementary Figure 2. For specifically-adhering GUVs that phase separate to form ordered-phase domains, the amount of ordered phase present is different than expected for free floating GUVs. A) The area fraction of ordered phase in the adhering area is roughly constant. Shown are data points and linear fits for three separate experiments. Experiment 1: Blue crosses and solid-lined fit with a slope of 0.39 ± 0.08 and $R^2 > 0.82$; Experiment 2: Grey crosses and dashed-lined fit with a slope of 0.31 ± 0.05 and $R^2 > 0.92$; Experiment 3: Red circles and dotted-lined fit with a slope of 0.19 ± 0.02 and $R^2 > 0.88$. The reported uncertainties are the 95% confidence intervals. B) Shown are histograms of the ordered-phase area fractions of the adhering area for the same three experiments as in panel (A), coded by the same colours. In contrast to the schematic in Figure 4A, the frequency distribution of ordered-phase area fractions in each experiment show a non-monotonic dependence on area fraction.

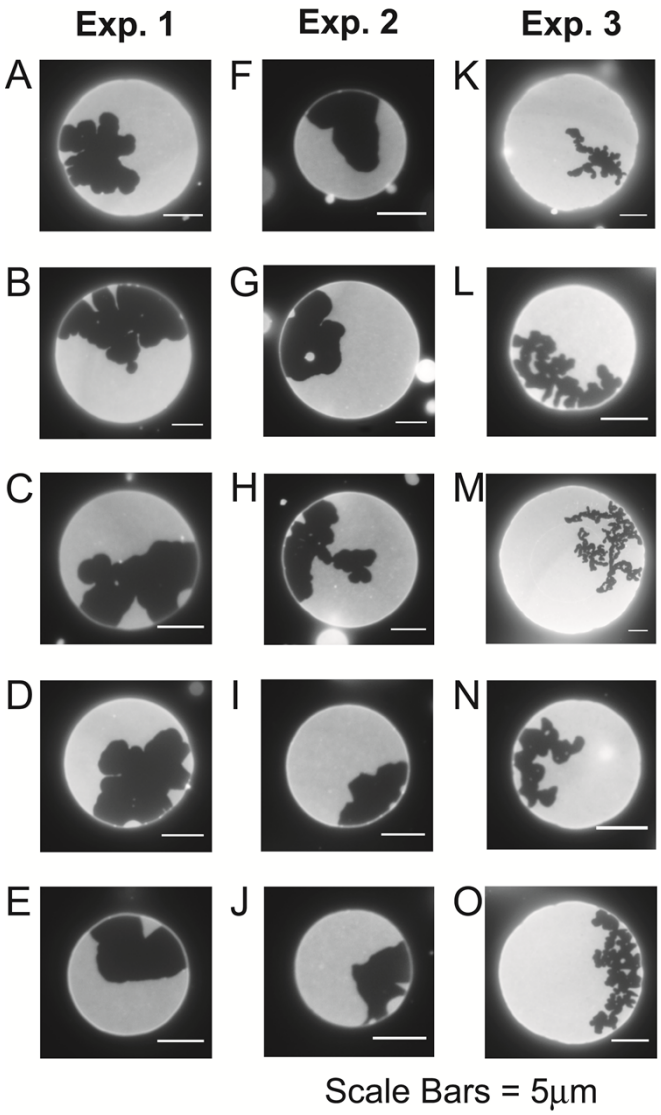

Supplemenary Figure 3. Catalogue of typical ordered domain shapes grouped by experiments numbered the same as in Supplementary Figure 1. Experiment 1 (A-E), Experiment 2 (F-J); Experiment 3 (K-O).

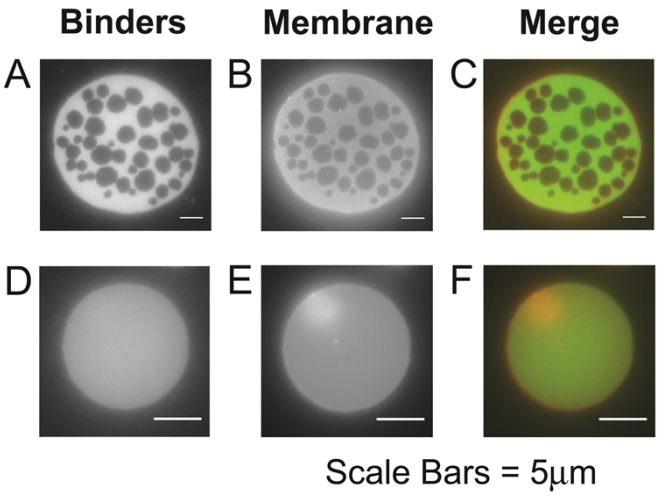

Supplementary Figure 4. Biotin-Neutravidin binders are excluded from ordered-phase domains and are uniformly distributed in adhering, disordered-phase regions in 21.5:21.5:57 DPPC:DiPhyPC:Cholesterol. Epifluorescent micrographs show, (A and D) fluorescently-labelled neutravidin (Oregon Green) and (B and E) the fluorescent disordered-phase marker DiI. These two spectrally-distinct channels are co-localized in both phase separated and non-phase separated vesicles as illustrated by false-colour merged images (C and F). Neutravidin is false-coloured green and DiI is false-coloured red.

Supplementary Table 1: DiI Enrichment in DiPhyPC Vesicles

30:20:50	DiPhyPC:DPPC:Cholesterol	1.5 ± 0.2
21.5:21.5:57	DiPhyPC:DPPC:Cholesterol	1.7 ± 0.2

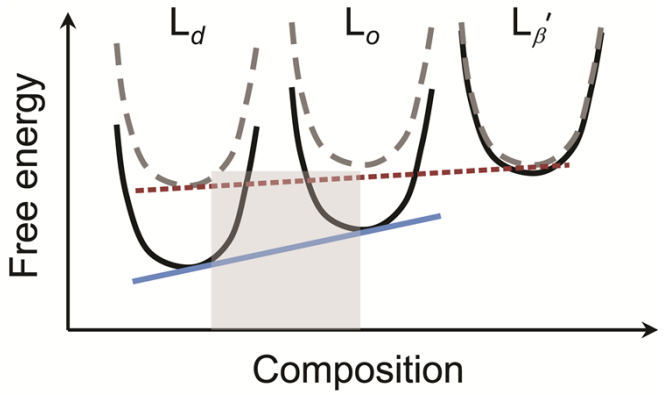

Supplementary Figure 5. A speculative free-energy schematic showing how adhesion could change equilibrium phase coexistence by differentially raising the free energies of different lipid phases. The free energies of non-adhering membrane phases L_d, L_o, and L_b' are shown as solid black curves. Membranes with compositions indicated by the grey square will minimize free energy by phase separating into L_d and L_o phases, as indicated by the solid blue common tangent line. The free energies of adhering membrane phases are shown as dashed grey curves. The L_o phase has been raised 80% as much as the L_d phase and the L_b' phase has been raised 10% as much. Now, membranes with compositions indicated by the grey square will minimize free energy by phase separating into L_d and L_b' phases, as indicated by the dotted red common tangent line.